⌘ *Author's Choice*

THE JOURNAL OF BIOLOGICAL CHEMISTRY VOL. 286, NO. 18, pp. 16386–16391, May 6, 2011


# Simplified Bacterial "Pore" Channel Provides Insight into the Assembly, Stability, and Structure of Sodium Channels*

Received for publication, February 24, 2011, and in revised form, March 13, 2011 Published, JBC Papers in Press, March 15, 2011, DOI 10.1074/jbc.C111.228122

**Emily C. McCusker‡, Nazzareno D'Avanzo§, Colin G. Nichols§, and B. A. Wallace‡1**

*From the ‡Department of Crystallography, Institute of Structural and Molecular Biology, Birkbeck College, University of London, London WC1E 7HX, United Kingdom and the §Department of Cell Biology and Physiology and Center for Investigation of Membrane Excitability Diseases, Washington University School of Medicine, St. Louis, Missouri 63110*

**Eukaryotic sodium channels are important membrane proteins involved in ion permeation, homeostasis, and electrical signaling. They are long, multidomain proteins that do not express well in heterologous systems, and hence, structure/function and biochemical studies on purified sodium channel proteins have been limited. Bacteria produce smaller, homologous tetrameric single domain channels specific for the conductance of sodium ions. They consist of N-terminal voltage sensor and C-terminal pore subdomains. We designed a functional pore-only channel consisting of the final two transmembrane helices, the intervening P-region, and the C-terminal extramembranous region of the sodium channel from the marine bacterium *Silicibacter pomeroyi*. This sodium "pore" channel forms a tetrameric, folded structure that is capable of supporting sodium flux in phospholipid vesicles. The pore-only channel is more thermally stable than its full-length counterpart, suggesting that the voltage sensor subdomain may destabilize the full-length channel. The pore subdomains can assemble, fold, and function independently from the voltage sensor and exhibit similar ligand-blocking characteristics as the intact channel. The availability of this simple pore-only construct should enable high-level expression for the testing of potential new ligands and enhance our understanding of the structural features that govern sodium selectivity and permeability.**

Voltage-gated sodium channels (VGSCs)[2] are membrane proteins responsible for rapid electrical signaling in eukaryotic organisms ranging from humans to electric eels to flies. In humans, VGSCs are current pharmaceutical targets for the treatment of pain (1), epilepsy (2), cardiovascular disease (3), and prostate (4) and breast (5) cancer. In prokaryotic organisms, VGSCs play vital roles in chemotaxis and homeostasis (6, 7). Our understanding of their mode of action, sodium selectivity, permeability, and the dynamics of how they achieve the different, distinct conformations that bind ligands is limited by the current lack of detailed structural information for this family of proteins.

Eukaryotic VGSCs are large (>200 kDa) monomeric heavily glycosylated membrane proteins composed of four pseudo-repeated domains, each of which contains six transmembrane segments that consist of a four-transmembrane (helices S1–S4)[3] N-terminal voltage sensor subdomain and a two-transmembrane (helices S5 and S6) C-terminal pore subdomain. Although they can be expressed in mammalian cells at the low levels necessary for electrophysiological studies, as of yet, there have been no reports of high-level expression in any systems in the quantities necessary for biophysical or structural characterization.

Bacterial VGSCs are simpler, being composed of shorter polypeptides, each consisting of a single six-transmembrane domain, that assemble as tetramers to form active channels. Since the identification of the first of these bacterial channels, NaChBac from *Bacillus halodurans* (8), a large related subfamily of bacterial sodium channels has been identified with high sequence similarities (7, 9–11). Electrophysiology studies following recombinant expression in mammalian cells have shown that the VGSCs $Na_vBP$ from *Bacillus pseudofirmus*, $Na_vSheP$ from *Shewanella putrefaciens*, $Na_vBacL$ from *Bacillus licheniformis*, $Na_vRosD$ from *Roseobacter denitrificans*, $Na_vsp$ from *Silicibacter pomeroyi,* and $Na_vpz$ from *Paracoccus zeaxanthinifaciens*, as well as NaChBac, are highly selective for $Na^+$ ions, bind calcium channel-blocking drugs, and exhibit activation, inactivation, and recovery similar to those of human sodium channels, albeit at ~10–100× slower rates (8, 9, 11). Bacterial VGSCs have ~20–25% identity with human VGSCs, but more importantly, have nearly identical hydrophobicity profiles and predicted topologies as each of the pseudo-repeated eukaryotic domains; therefore they are expected to have similar overall structures. High-level bacterial expression, purification, and characterization of NaChBac and a thermally stabilized mutant of this channel have been described (12, 13).

VGSCs are members of the same family as voltage-gated potassium channels, for which there are a number of crystal structures available (14–16). In those channels, the two subdomains appear to be spatially independent. Recent studies using disulfide cross-linking to trap regions of proximity (17) suggest that NaChBac forms a similar three-dimensional

* This work was supported by a project grant from the Biotechnology and Biological Science Research Council (BBSRC) (to B. A. W.) and a BBSRC SPORT programme grant to the Membrane Protein Structure Initiative consortium (to N. Isaacs, principal investigator). This work was supported in part by National Institutes of Health Grant HL54171 (to C. G. N.).

⌘ *Author's Choice*—Final version full access.

[1] To whom correspondence should be addressed: Birkbeck College, University of London, Malet St., London, UK. Fax: 44-207-631-6803; E-mail: b.wallace@mail.cryst.bbk.ac.uk.

[2] The abbreviations used are: VGSC, voltage-gated sodium channel; DM, decyl maltoside; $Na_vsp$, full-length sodium channel from *S. pomeroyi*; sp-pore, pore-only construct; SRCD, synchrotron radiation circular dichroism; Ni-NTA, nickel-nitrilotriacetic acid; NMG, *N*-methyl-D-glucamine.

[3] S1–S6 are designations for the transmembrane segments numbered beginning at the N terminus.

arrangement to the voltage-gated potassium channels. The pore subdomains form a compact central transmembrane pathway capable of accommodating ions in both selectivity and cavity regions; this is surrounded by the relatively loosely associated voltage sensor subdomains. Isolation and expression of the N-terminal four-transmembrane voltage sensor subdomain of the NaChBac channel (17) showed that the voltage sensor alone was capable of folding in the absence of the pore subdomain, and EPR measurements confirmed that it has a more tightly packed but similar overall fold to that of potassium voltage sensors (18). Here we designed a pore-only version of the $Na_vsp$ bacterial sodium channel and investigated whether it formed folded, stable tetramers and was capable of supporting $Na^+$-specific ion channel permeability in the absence of the voltage sensor.

## EXPERIMENTAL PROCEDURES

*Materials*—The prokaryotic homologue gene isolated from *S. pomeroyi* was supplied by Prof. David E. Clapham (Howard Hughes Medical Institute, Children's Hospital, Harvard Medical School, Boston, MA) (9). Quick ligase, restriction enzymes, and DH5$\alpha$ chemically competent cells were purchased from New England Biolabs. Syntheses of PCR primers and all DNA sequencing were performed by Eurofins MWG Operon. Ni-NTA and all DNA purification supplies were purchased from Qiagen, Inc. Thrombin and the pET15b vector were purchased from Novagen, Inc. (EMD Chemicals, Darmstadt, Germany). Decyl maltoside detergent (DM) was obtained from Anatrace, Inc., and lipids were from Avanti Polar Lipids, Inc. Unless otherwise noted, chemicals were obtained from Sigma-Aldrich.

*Cloning Expression Constructs*—The pore-only construct (see Fig. 1, *gray residues*), composed of the C-terminal region beginning at transmembrane helix 5, was designed based on multiple sequence alignment (ClustalW (19)) across the family of prokaryotic voltage-gated sodium channels and with the MlotiK, Kv1.2-Kv2.1 chimera, and KcsA potassium channel crystal structures (PDB codes 3beh, 2r9r and 1bl8, respectively) (14, 16, 20). Dictionary of Protein Secondary Structure (DSSP) (21) analyses of the crystal structures via the 2Struc server (22) were use to define the ends of the helical regions. The full-length construct ($Na_vsp$) and the pore-only construct (sp-pore) were PCR-amplified to incorporate an N-terminal NdeI site and a C-terminal BamHI site using the following primers: $Na_vsp$ forward primer, 5′-GGAGAAATTACATATGGGACAAAGAATG-3′, and reverse primer, 5′-CCCTGAAAATACGGATCCTACTTTTTGGT-3′; sp-pore forward primer, 5′-TGCGCTGCCCCATATGGCCAGCGTG-3′, and reverse primer, 5′-GTTAGCAGCCGGATCCTACTTTTTGG-3′. These restriction sites enabled simple restriction digest and ligation into the pET15b vector. Both constructs were transformed into C41(DE3) cells for expression.

*Expression and Purification*—5 $\mu$l of LB medium (containing 50 $\mu$g/ml ampicillin) was inoculated from a single colony and grown for 8 h at 37 °C. 100 $\mu$l of LB medium containing ampicillin (50 $\mu$g/ml) was inoculated with 100 $\mu$l of culture and grown overnight at 30 °C. The overnight culture was used to inoculate 6 liters of LB medium containing ampicillin (50 $\mu$g/ml). Cultures were grown at 37 °C until an $A_{600}$ of 0.6, at which time isopropyl-$\beta$-D-thiogalactopyranoside was added to a final concentration of 500 $\mu$M. Cultures were harvested 4 h after induction via centrifugation at 6,000 $\times$ *g* at 4 °C. All cell pellets were stored at −80 °C.

Cell pellets were suspended in TBS (20 mM Tris, pH 7.5, 150 mM NaCl) buffer supplemented with 0.2 mM of the protease inhibitor phenylmethanesulfonyl fluoride (VWR International) and 2 $\mu$g/ml DNase I and 2.5 mM $MgSO_4$ and lysed by cell disruption using an Avestin EmulsiFlex-C5. The lysate was centrifuged at 10,000 $\times$ g for 30 min to pellet unlysed cells and insoluble cellular debris. The supernatant was centrifuged at 43,000 $\times$ *g* for 1 h to pellet membranes. The membranes were resuspended in TBS with 50 mM decyl maltoside and incubated at 4 °C for 4 h.

Approximately 1.5 ml of Ni-NTA slurry was equilibrated with TBS buffer and added to the solubilized membranes from a 6-liter culture. Histidine-tagged proteins were allowed to bind overnight at 4 °C. Solubilized membranes containing Ni-NTA resin were spun down at 2,000 $\times$ *g* for 5 min, and buffer was poured off. The resin was resuspended three times in TBS, 0.2% DM, 300 mM NaCl, containing progressively 25, 30, and 35 mM imidazole, for 0.5 h each to wash away non-specifically bound proteins. Four consecutive elutions, at 4 ml each, were performed in TBS with 0.2% DM and 300 mM imidazole. Elutants were checked for purity on SDS-PAGE and combined. These were then filtered using a 0.22-$\mu$m filter and concentrated using an Amicon ultrafiltration device (50-kDa molecular mass cutoff for sp-pore and 100 kDa for $Na_vsp$, respectively) prior to thrombin cleavage. During concentration, imidazole was removed via buffer exchange. Thrombin cleavage took place at room temperature overnight at 20 units/4 mg of protein. The cleaved protein, cleaved His tag, and remaining His-tagged protein were incubated with Ni-NTA, and the flow-through was collected.

*Gel Filtration Chromatography*—The Ni-NTA flow-through was filtered through a 0.22-$\mu$m filter and then concentrated in preparation for loading onto a gel filtration column. Gel filtration (Superdex 200 10/300 GL, GE Healthcare) was used to isolate the predicted tetrameric channel. Protein was eluted with 10 mM Tris-HCl, pH 7.5, 100 mM NaCl, 0.02% $NaN_3$, and 0.2% DM at a rate of 0.5 ml/min.

*Circular Dichroism (CD) Spectroscopy*—Synchrotron radiation circular dichroism (SRCD) spectra were collected on the CD1 beamline at the Institute for Storage Ring Facilities in Aarhus (ISA) Synchrotron, Aarhus, Denmark. For all CD measurements, the protein concentrations were determined immediately prior to measurement. The beamline was calibrated with camphorsulfonic acid at the beginning of the data collection. The extinction coefficient at 280 nm was calculated from the amino acid sequence using the ExPASy ProtParam website (23), and the concentration was determined from the $A_{280}$ measured on a Nanodrop 1000 UV spectrophotometer.

$Na_vsp$ (5.7 mg/ml) or sp-pore (5 mg/ml) in the gel filtration buffer was loaded into a 0.009-mm path length quartz Suprasil demountable cell (Hellma UK Ltd.), and three spectra were collected at 25 °C over the wavelength range from 280 to 170 nm,

with a 1-nm step size and a 2-s dwell time. The replicates were averaged, and the averaged baselines (consisting of the buffer, including detergent but no protein) were subtracted from the averaged sample spectra. Data processing was carried out with the CDtool software (24), using mean residue weights of 112.3 and 113.9 for $Na_vsp$ and sp-pore, respectively. Data were analyzed with the DichroWeb analysis server (25); the reported values were the averaged results using three different algorithms (CONTINLL (26, 27), SELCON3 (28), and CDDSTR (28)) and the SP175t reference dataset (29). The goodness-of-fit parameters for both samples were $<0.08$, indicating reliable analyses.

Thermal melts were undertaken using an Aviv 62ds spectropolarimeter with a detector acceptance angle of >90° (for membrane/scattering samples). Two thermal denaturation experiments were performed for each protein sample using a 0.1-mm path length Suprasil cuvette. Measurements were made on samples at >1 mg/ml at the wavelength 222 nm using set temperature interval steps of 5 °C between 15 and 100 °C. The actual sample temperature (as opposed to the set temperature) was determined using a thermistor probe inserted in the sample cell. An equilibration time of 3 min was used at each temperature point. Melting curves were produced using a two-parameter Boltzmann sigmoidal fit function in SciDAVis (Scientific Data Analysis and Visualization).

*$^{22}Na^+$ Uptake Assay*—1-Palmitoyl-2-oleoyl-3-phosphatidylethanolamine and liver L-α-phosphatidylinositol were solubilized in buffer A (450 mM NaCl, 10 mM HEPES, 4 mM NMG, pH 7.5) with 35 mM CHAPS at 10 mg/ml, mixed in a 3:1 ratio, and incubated at room temperature for 2 h. Polystyrene columns (Pierce) were packed with Sephadex G-50 beads, presoaked overnight in buffer A, and spun on a Beckman TJ6 centrifuge until reaching 3,000 rpm. 20 μg of $Na_vsp$ or 30 μg of sp-pore protein was added to 100 μl of lipid (1 mg) and incubated for 30 min. Liposomes were formed by adding the protein/lipid sample to the partially dehydrated columns and spinning to 2,500 rpm. The extra-liposomal solution was exchanged by spinning the sample to 2,500 rpm in partially dehydrated columns, now containing beads soaked in buffer B (400 mM sorbitol, 10 mM HEPES, 4 mM NMG, pH 7.5). $^{22}Na^+$ uptake was initiated by adding 400 μl of buffer B containing $^{22}Na^+$ and the indicated concentration of mibefradil. The addition of mibefradil to buffer B at concentrations greater than 500 μM rapidly induced a thick precipitate even before being added to the proteoliposomes and thus could not screened. At various time points, aliquots of the liposome uptake reaction were flowed through 0.5-ml Dowex cation exchange columns charged with NMG in protonated form to remove extra-liposomal $^{22}Na^+$. These aliquots were then mixed with scintillation fluid and counted in a liquid scintillation counter. Fractional flux at 60 min in the presence of mibefradil was determined following data subtraction from uptake counts measured at each time point from protein-free liposomes.

## RESULTS

*Construct Design and Protein Expression and Purification*—Sequence alignments were used to predict the locations of the six transmembrane segments of the $Na_vsp$ channel (Fig. 1).

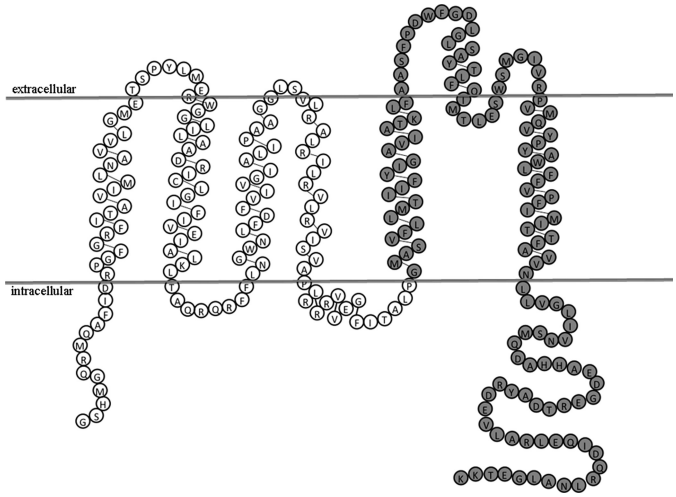


FIGURE 1. **Primary structure of full-length $Na_vsp$ and sp-pore (*gray residues*) constructs.**

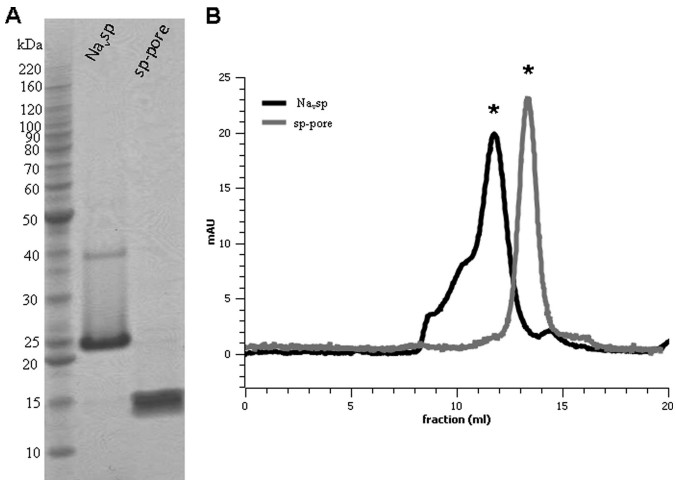


FIGURE 2. **Purification and isolation of tetrameric $Na_vsp$ and sp-pore.** *A*, $Na_vsp$ and sp-pore migrate as monomers of ~25 and 15 kDa, respectively, on SDS-PAGE. *B*, $Na_vsp$ and sp-pore elute as tetramers from a Superdex 200 gel filtration column after purification in 0.2% DM. The peaks positions indicated with an *asterisk* correspond to ~155 kDa for $Na_vsp$ and ~92 kDa for sp-pore, respectively.

Numerous key residues, such as the voltage-sensing charges on S4 and the residues involved with ion selectivity, were used to confirm the sequence alignment. The minimal pore construct designed (Fig. 1, *gray residues*) included only S5, the S5-S6 P-linker with the proposed selectivity filter, S6, and the C-terminal domain that is predicted to form a coiled-coil domain when the four subunits associate (10).

Both $Na_vsp$ and sp-pore were readily expressed (at similar levels) in *Escherichia coli*, and roughly comparable yields of the solubilized purified proteins were produced. The purified $Na_vsp$ and sp-pore proteins migrate in SDS denaturing gels near their predicted monomeric molecular masses (~29 and 15 kDa, respectively) (Fig. 2*A*). The slightly higher value than predicted for $Na_vsp$ (~25 kDa) is commonly seen for membrane proteins that have reduced SDS solvation (30). Western blot analyses suggest that the small higher molecular weight band for $Na_vsp$ is likely to be a dimer.

*Quaternary Structure Analysis*—Both protein constructs eluted at the predicted tetrameric size ($Na_vsp$ ~155 kDa and

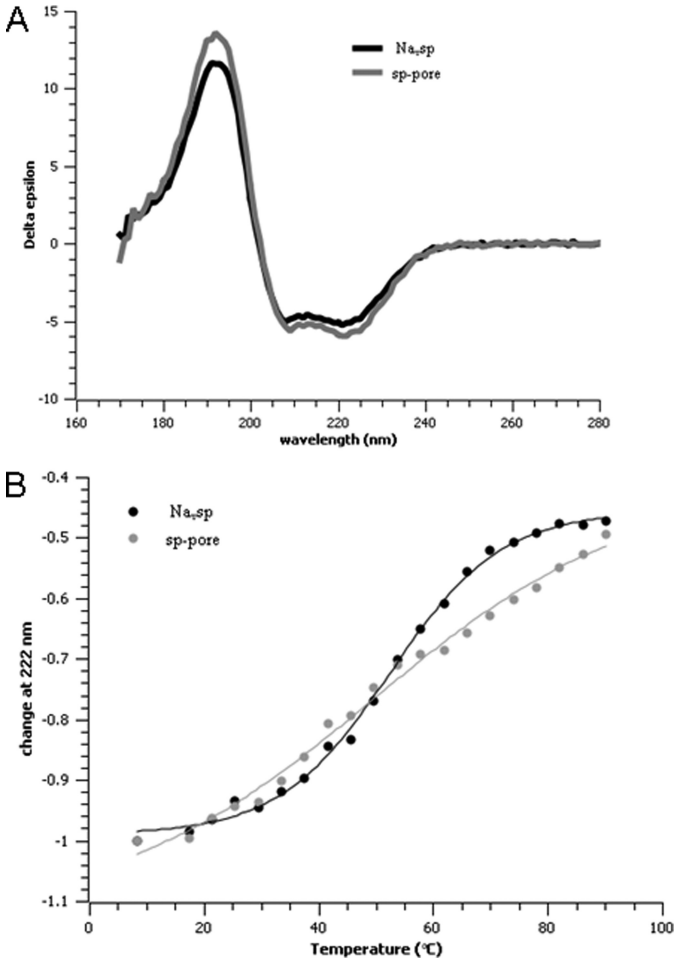


FIGURE 3. **Secondary structures and thermal stabilities.** *A*, synchrotron radiation circular dichroism spectra of $Na_vsp$ (*black*) and sp-pore (*gray*) tetramers in decyl maltoside. *B*, thermal melts using CD spectroscopy monitored at 222 nm ($Na_vsp$ in *black* and sp-pore in *gray*).

sp-pore ~92 kDa), which are the molecular masses of the protein tetramers plus the approximate mass of a DM micelle (~33 kDa) (Fig. 2*B*) in the presence of sodium ions. No monomers were evident. In the absence of sodium ions or in the presence of other monovalent cations, tetramers are destabilized, with the pore construct being less stable than the full-length construct (data not shown).

*Secondary Structure Determination*—The secondary structures of both $Na_vsp$ and sp-pore in DM were examined using SRCD spectroscopy. This method was used rather than conventional CD spectroscopy to enable the collection of low wavelength data in the detergent-containing buffer and more accurate analyses of the proteins. $Na_vsp$ and sp-pore tetramers have spectra typical of folded $\alpha$ helical-rich proteins (with the pore having the appearance of a slightly more helical structure due to the larger magnitudes of its peaks at ~190, 208, and 222 nm) (Fig. 3*A*). The secondary structures of $Na_vsp$ and sp-pore were calculated to be 52 and 55% helical, respectively. The estimated helix content for the sp-pore based on the homology model is ~56%, a close match to the calculated value. The helical regions in the voltage sensor are less well aligned with potassium sequences, so it is more difficult to predict their extent and thus the precise secondary structure content of the whole channel. However, it is clear that it should be slightly lower percentage-wise than the sp-pore due to the less extensive helical nature of S4 and the five non-helical extramembranous segments (four loops and the N terminus). Hence, the 52% helix measured for the intact protein is in line with what would be expected. These measurements thus indicate that both proteins are folded with well ordered, mostly helical secondary structures.

*Stability in Vitro*—The overall thermal stabilities of $Na_vsp$ and sp-pore were compared by monitoring the unfolding of the proteins using circular dichroism spectroscopy. The secondary structures (specifically the helical components monitored at 222 nm) of both proteins indicated that the proteins unfolded with two-state profiles and that the channel had a lower $T_m$ than the pore (Fig. 3*B*). The unfolding was irreversible for both constructs. The $T_m$ calculated for $Na_vsp$ was 58 °C. However, the $T_m$ for the pore could not be accurately measured as it had clearly not completed unfolding even at >90 °C. The pore retained a residual helical content of ~30% helix at this temperature, whereas the corresponding residual helical structure of the channel was only 19%. Taken together, these results indicate that the pore-only construct was considerably more thermally stable than the full-length protein and suggest either that the voltage sensor subdomain was more thermally labile itself or that it imparted an instability/flexibility to the intact protein.

*Activity*—Sodium influx was measured in the presence and absence of the calcium channel blocker (mibefradil) previously shown to be effective against bacterial VGSCs. Both $Na_vsp$ and sp-pore demonstrated sodium permeability (Fig. 4, *A* and *B*). The addition of greater than 100 $\mu$M mibefradil reduced $Na^+$ flux in both proteins by ~50% (Fig. 4*C*). This is similar to the level of mibefradil inhibition observed in NaChBac assessed by sodium green fluorescence (12). Thus, both the full-length and the pore-only proteins were capable of forming the correct pore arrangements required for $Na^+$ channel activity.

## DISCUSSION

In an attempt to make a minimal functional sodium channel based on a bacterial VGSC, we designed and constructed a pore-only version of the $Na_vsp$ channel. The notion that this could be possible arose from the naturally occurring KcsA potassium channel (20, 31), which contains only two-transmembrane helices and shows strong topological similarities with the $Na_vsp$ channel. In addition, various six-transmembrane potassium channel structures have shown a wide diversity in the geometries of the interactions between the pore and voltage sensor subdomains (14–16), and it has been shown that it is possible to create a monomeric standalone voltage sensor subdomain of a bacterial VGSC (17). These all suggested that the voltage sensor and pore subdomains might both fold and function relatively independently, and hence, a pore-only channel might be viable. Chen *et al.* (32) showed that it was possible to express a "minimal" eukaryotic sodium channel in mammalian cells consisting of four two-transmembrane regions tethered together; this protein exhibited toxin binding but did not conduct sodium currents. We sought to design and purify an even simpler functional bacterial sodium pore and compare its *in vitro* properties with that of the cognate full-length channel.

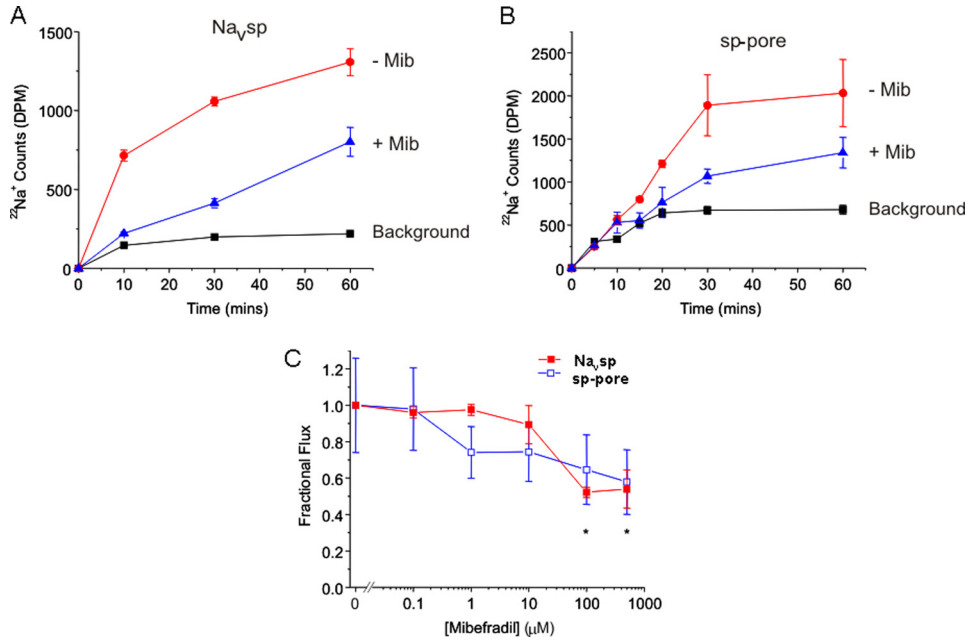


FIGURE 4. **Sodium flux activities of Na$_v$sp and sp-pore.** *A*, representative time course of $^{22}Na^+$ uptake into 3:1 1-palmitoyl-2-oleoyl-3-phosphatidylethanolamine L-α-phosphatidylinositol liposomes reconstituted with full-length Na$_v$sp in the absence (*circles*) and presence (*triangles*) of mibefradil. Background $^{22}Na^+$ into protein-free liposomes is shown for comparison (*squares*) ($n = 6$). *B*, same as in *A*, except that sp-pore was reconstituted instead ($n = 5$). *C*, concentration dependence of mibefradil block at 60 min in Na$_v$sp (*closed squares*) and sp-pore (*open squares*). In all cases, the lines are simply connections between the data points rather than theoretical fits to any model; any apparent differences between the curves are within the experimental errors of the measurements. The *asterisks* denote significance (*, $p < 0.05$) at those concentrations for both proteins relative to 0 μM mibefradil. *Error bars* indicate S.E.

The aim was to create a minimalistic channel that would be suitable for biochemical, structural, functional, and computational (molecular dynamics) studies and for pore-blocking ligand binding studies and that could be used to test the hypothesis that the pore subdomain is capable of folding and functioning separately of the voltage sensor.

The full-length Na$_v$sp channel and the sp-pore both formed stable tetramers following isolation and purification in the mild non-ionic detergent DM in the presence of NaCl. The sp-pore was tetrameric in the absence of the voltage sensor subdomain, which suggests that the association between monomers in the channel is largely mediated at the interfaces between the S5 and S6 transmembrane segments. Isolated voltage sensor domains do not assemble as tetramers (17, 18). It is therefore likely that the pore region (including its C terminus) is pivotal for forming the tetramers in the intact channels.

Circular dichroism spectroscopy has demonstrated that both the full-length and the sp-pore are folded structures and that sp-pore is exceptionally stable under heat treatment. The reason for this stability may be because the central core includes intimate helix-helix interactions in the transmembrane region (a structural feature that has been shown to be highly resistant to thermal unfolding in model systems (33)). The pore-only construct also contains the large C-terminal region, which has been shown to be helical (10) and has been proposed to form a coiled-coil structure, which although not required for tetramer stability (34) may be important for initial tetramer assembly (10, 34). The lower overall helical content found for the full-length channel suggests that on average, it contains less ordered secondary structure, which might suggest some flexibility in the voltage sensor loops and N-terminal region. This may be further reflected in its loss of ordered structure at a lower temperature than in the pore.

After reconstitution, both the full-length Na$_v$sp and the sp-pore were able to support sodium ion flux, which was blockable by the ligand mibefradil. This ligand is believed to bind in the permeability pathway, and hence, because its efficacy is maintained in the pore, this further suggests that the central ion binding region is properly folded in the pore construct.

In summary, these studies have indicated that the pore subdomain alone is capable of functioning as a channel and that the selectivity filter and permeability pathways are correctly folded. This is evidence that the pore-only protein is very similar to the pore structure when it is associated with the voltage sensor and suggests this simple channel could be an important tool for elucidating the structural basis of sodium channel activity and the design and screening of potential new pore-blocking drugs.

*Acknowledgments—Access to the CD1 beamline at the ISA Synchrotron is acknowledged under the European Union (EU) Integrated Infrastructure Initiative (I3), Integrated Activity on Synchrotron and Free Electron Laser Science (IA-SFS), Contract Number RII3-CT-2004-506008. We thank Dr. Andrew J. Miles for help with the SRCD data collection and for helpful discussions.*

## REFERENCES

1. Jarvis, M. F., Honore, P., Shieh, C. C., Chapman, M., Joshi, S., Zhang, X. F., Kort, M., Carroll, W., Marron, B., Atkinson, R., Thomas, J., Liu, D., Krambis, M., Liu, Y., McGaraughty, S., Chu, K., Roeloffs, R., Zhong, C., Mikusa, J. P., Hernandez, G., Gauvin, D., Wade, C., Zhu, C., Pai, M., Scanio, M., Shi, L., Drizin, I., Gregg, R., Matulenko, M., Hakeem, A., Gross, M., Johnson, M., Marsh, K., Wagoner, P. K., Sullivan, J. P., Faltynek, C. R., and Krafte,

D. S. (2007) *Proc. Natl. Acad. Sci. U.S.A.* **104,** 8520–8525
2. Liu, Y., Yohrling, G. J., Wang, Y., Hutchinson, T. L., Brenneman, D. E., Flores, C. M., and Zhao, B. (2009) *Epilepsy Res.* **83,** 66–72
3. Zimmer, T., and Surber, R. (2008) *Prog. Biophys. Mol. Biol.* **98,** 120–136
4. Anderson, J. D., Hansen, T. P., Lenkowski, P. W., Walls, A. M., Choudhury, I. M., Schenck, H. A., Friehling, M., Höll, G. M., Patel, M. K., Sikes, R. A., and Brown, M. L. (2003) *Mol. Cancer Ther.* **2,** 1149–1154
5. Fraser, S. P., Diss, J. K., Chioni, A. M., Mycielska, M. E., Pan, H., Yamaci, R. F., Pani, F., Siwy, Z., Krasowska, M., Grzywna, Z., Brackenbury, W. J., Theodorou, D., Koyutürk, M., Kaya, H., Battaloglu, E., De Bella, M. T., Slade, M. J., Tolhurst, R., Palmieri, C., Jiang, J., Latchman, D. S., Coombes, R. C., and Djamgoz, M. B. (2005) *Clin. Cancer Res.* **11,** 5381–5389
6. Fujinami, S., Terahara, N., Krulwich, T. A., and Ito, M. (2009) *Future Microbiol.* **4,** 1137–1149
7. Ito, M., Xu, H., Guffanti, A. A., Wei, Y., Zvi, L., Clapham, D. E., and Krulwich, T. A. (2004) *Proc. Natl. Acad. Sci. U.S.A.* **101,** 10566–10571
8. Ren, D., Navarro, B., Xu, H., Yue, L., Shi, Q., and Clapham, D. E. (2001) *Science* **294,** 2372–2375
9. Koishi, R., Xu, H., Ren, D., Navarro, B., Spiller, B. W., Shi, Q., and Clapham, D. E. (2004) *J. Biol. Chem.* **279,** 9532–9538
10. Powl, A. M., O'Reilly, A. O., Miles, A. J., and Wallace, B. A. (2010) *Proc. Natl. Acad. Sci. U.S.A.* **107,** 14064–14069
11. Irie, K., Kitagawa, K., Nagura, H., Imai, T., Shimomura, T., and Fujiyoshi, Y. (2010) *J. Biol. Chem.* **285,** 3685–3694
12. Nurani, G., Radford, M., Charalambous, K., O'Reilly, A. O., Cronin, N. B., Haque, S., and Wallace, B. A. (2008) *Biochemistry* **47,** 8114–8121
13. O'Reilly, A. O., Charalambous, K., Nurani, G., Powl, A. M., and Wallace, B. A. (2008) *Mol. Membr. Biol.* **25,** 670–676
14. Clayton, G. M., Altieri, S., Heginbotham, L., Unger, V. M., and Morais-Cabral, J. H. (2008) *Proc. Natl. Acad. Sci. U.S.A.* **105,** 1511–1515
15. Jiang, Y., Lee, A., Chen, J., Ruta, V., Cadene, M., Chait, B. T., and MacKinnon, R. (2003) *Nature* **423,** 33–41
16. Long, S. B., Tao, X., Campbell, E. B., and MacKinnon, R. (2007) *Nature* **450,** 376–382
17. Chakrapani, S., Sompornpisut, P., Intharathep, P., Roux, B., and Perozo, E. (2010) *Proc. Natl. Acad. Sci. U.S.A.* **107,** 5435–5440
18. Shimomura, T., Irie, K., Nagura, H., Imai, T., and Fujiyoshi, Y. (2011) *J. Biol. Chem.* **286,** 7409–7417
19. Larkin, M. A., Blackshields, G., Brown, N. P., Chenna, R., McGettigan, P. A., McWilliam, H., Valentin, F., Wallace, I. M., Wilm, A., Lopez, R., Thompson, J. D., Gibson, T. J., and Higgins, D. G. (2007) *Bioinformatics* **23,** 2947–2948
20. Doyle, D. A., Morais Cabral, J., Pfuetzner, R. A., Kuo, A., Gulbis, J. M., Cohen, S. L., Chait, B. T., and MacKinnon, R. (1998) *Science* **280,** 69–77
21. Kabsch, W., and Sander, C. (1983) *Biopolymers* **22,** 2577–2637
22. Klose, D. P., Wallace, B. A., and Janes, R. W. (2010) *Bioinformatics* **26,** 2624–2625
23. Gasteiger, E., Gattiker, A., Hoogland, C., Ivanyi, I., Appel, R. D., and Bairoch, A. (2003) *Nucleic Acids Res.* **31,** 3784–3788
24. Lees, J. G., Smith, B. R., Wien, F., Miles, A. J., and Wallace, B. A. (2004) *Anal. Biochem.* **332,** 285–289
25. Whitmore, L., and Wallace, B. A. (2008) *Biopolymers* **89,** 392–400
26. Provencher, S. W., and Glöckner, J. (1981) *Biochemistry* **20,** 33–37
27. van Stokkum, I. H., Spoelder, H. J., Bloemendal, M., van Grondelle, R., and Groen, F. C. (1990) *Anal. Biochem.* **191,** 110–118
28. Sreerama, N., and Woody, R. W. (2000) *Anal. Biochem.* **287,** 252–260
29. Lees, J. G., Miles, A. J., Wien, F., and Wallace, B. A. (2006) *Bioinformatics* **22,** 1955–1962
30. Rath, A., Glibowicka, M., Nadeau, V. G., Chen, G., and Deber, C. M. (2009) *Proc. Natl. Acad. Sci. U.S.A.* **106,** 1760–1765
31. Cuello, L. G., Jogini, V., Cortes, D. M., Pan, A. C., Gagnon, D. G., Dalmas, O., Cordero-Morales, J. F., Chakrapani, S., Roux, B., and Perozo, E. (2010) *Nature* **466,** 272–275
32. Chen, Z., Alcayaga, C., Suarez-Isla, B. A., O'Rourke, B., Tomaselli, G., and Marban, E. (2002) *J. Biol. Chem.* **277,** 24653–24658
33. Ulmschneider, M. B., Doux, J. P., Killian, J. A., Smith, J. C., and Ulmschneider, J. P. (2010) *J. Am. Chem. Soc.* **132,** 3452–3460
34. Mio, K., Mio, M., Arisaka, F., Sato, M., and Sato, C. (2010) *Prog. Biophys. Mol. Biol.* **103,** 111–121